genesis 54:212–219 (2016)

TECHNOLOGY REPORT

Automated Analysis of Sleep Control via a Single Neuron Active at Sleep Onset in *C. elegans*

Birk Urmersbach, Judith Besseling, Jan-Philipp Spies, and Henrik Bringmann*

Max Planck Institute for Biophysical Chemistry, Am Fassberg 11, Goettingen, 37077, Germany

Received 2 December 2015; Revised 27 January 2016; Accepted 28 January 2016

Summary: Longitudinal analyses are crucial for understanding long-term processes such as development and behavioral rhythms. For a complete understanding of such processes, both organism-level observations as well as single-cell observations are necessary. Sleep is an example for a long-term process that is under developmental control. This behavioral state is induced by conserved sleep-active neurons, but little is known about how sleep neurons control the physiology of an animal systemically. In the nematode *C. elegans*, sleep induction crucially requires the single RIS interneuron to actively induce a developmentally regulated sleep behavior. Here, we used RIS-induced sleep as an example of how longitudinal analyses can be automated. We developed methods to analyze both behavior and neural activity in larva across the sleep-wake cycle. To image behavior, we used an improved DIC contrast to extract the head and detect the nose. To image neural activity, we used GCaMP3 expression in a small number of neurons including RIS combined with a neuron discrimination algorithm. Thus, we present a comprehensive platform for automatically analyzing behavior and neural activity in *C. elegans* exemplified by using RIS-induced sleep during *C. elegans* development. genesis 54:212–219, 2016. © 2016 Wiley Periodicals, Inc.

Key words: Caenorhabditis elegans; sleep; sleep-active neuron; behavior

INTRODUCTION

Sleep is an essential behavior that is found in animals that have a nervous system (Cirelli and Tononi, 2008). It is intimately linked to development: sleep is controlled by development and sleep is required for developmental processes. In most species, developing individuals sleep more than adults (Roffwarg *et al*., 1966). Sleep is defined by behavioral criteria such as the absence of voluntary movement, an increased arousal threshold, a specific posture and homeostatic regulation (Campbell and Tobler, 1984). In mammals, sleep is induced by sleep-active sleep-promoting neurons that express GABA and neuropeptides (Saper *et al*., 2005). However, little is known about the control of sleep neurons and the induction of sleep.

C. elegans has emerged as a model for studying developmentally regulated sleep behavior, as it displays various types of quiescence behavior both in the adult as well as in the larva. Adult worms show a behavior called "satiety quiescence" that is dependent on the nutritional state of the animal and the quality of the food (You *et al*., 2008). In addition, adults can engage in a quiescent state following stress (Hill *et al*., 2014). Whereas adult quiescence in *C. elegans* is highly dependent on environmental conditions (You *et al*., 2008), larvae show a highly determined quiescence behavior that is coupled to the molting cycle. At the end of each of the four molts, larvae display a quiescent phase called lethargus that lasts about 2 h (Cassada and Russell, 1975). This behavior fulfills the behavioral criteria that define sleep in higher organisms and has thus been called sleep-like (Iwanir *et al*., 2013; Raizen *et al*., 2008; Schwarz *et al*., 2011). Although initially, the relationship of *C. elegans* sleep-like behavior and mammalian sleep had been unclear, subsequent molecular dissection reveals related control mechanisms, suggesting that these seemingly disparate behaviors evolved

*Correspondence to: Max Planck Institute for Biophysical Chemistry, Am Fassberg 11, Goettingen 37077, Germany.
E-mail: Henrik.Bringmann@mpibpc.mpg.de
Published online 7 April 2016 in
Wiley Online Library (wileyonlinelibrary.com).
DOI: 10.1002/dvg.22924

from a common ancestral sleep state (Jeon *et al*., 1999; Singh *et al*., 2014; Turek *et al*., 2013; Van Buskirk and Sternberg, 2007). *C. elegans* is a powerful system for molecular dissection of biological processes as it is amenable to molecular genetics, is transparent, and has a defined and invariant nervous system. Through analysis of a sleep mutant in *C. elegans* a crucial neuron for sleep induction, called RIS, was identified. RIS is active at the onset of sleep, actively induces sleep, and expresses GABA and neuropeptides (Turek *et al*., 2013). Thus, RIS likely is the counterpart to sleep neurons in mammals. Because it is just one neuron in a well-characterized model system, the mechanisms of sleep induction by this neuron can be easily analyzed.

Because sleep is defined by behavioral criteria, analysis of behavior is essential for characterizing sleep mutants and for dissecting the sleep mechanism. The behavior of larvae can be imaged and sleep behavior, as defined by locomotion absence, can be assessed (Bringmann, 2011; Nagy *et al*., 2014; Raizen *et al*., 2008; Schwarz and Bringmann, 2013; Turek *et al*., 2015; Van Buskirk and Sternberg, 2007). As the sleep-wake cycle is a process that takes several hours, large datasets need to get analyzed. Ideally, the behavioral analysis gives an absolute readout of both immobility phases as well as mobility phases including wake. This is important because the absolute quiescence time is greatly dependent on general activity levels and many mutants have been shown to have unspecific changes in quiescence and changes in baseline activity. While frame-subtraction algorithms are useful for extracting absolute quiescence they do not provide a quantifiable measure for mobile behavior (Nagy *et al*., 2014; Raizen *et al*., 2008; Singh *et al*., 2014). Tracking animal centroids or nose movement has proven useful for quantifying quiescence in older larvae or adults (Bringmann, 2011; Turek *et al*., 2015; Van Buskirk and Sternberg, 2007). The ultimate goal of behavioral analysis should be elaborated tracking of the entire worm outline, which has lead to a quantitative understanding of behavior in wild type and many mutants (Yemini *et al*., 2013). Small *C. elegans* larvae, however, provide little imaging contrast and thus automated tracking programs are not available for analyzing their behavior yet. Developing automated image analysis algorithms for small larvae is desirable because the small larvae have a unique biology and allow an excellent functional neural imaging (Cho and Sternberg, 2014; Nagy *et al*., 2014; Schwarz *et al*., 2011, 2012; Turek *et al*., 2015).

Sleep behavior is controlled by neurons and thus analyzing neural activity is required for understanding sleep behavior. Functional neural imaging using genetically encoded calcium indicators has been straightforward in *C. elegans*, as these sensors can be expressed specifically in neurons of interest and fluorescence can be imaged noninvasively in the transparent worm (Kerr *et al*., 2000). Because of their large dynamic range, GCaMP sensors have been extremely useful in this system (Kerr, 2006). Given that calcium transients typically last only several seconds, near-continuous calcium imaging needs to be performed over several hours, resulting in thousands of image frames that need to get analyzed.

Here we provide a system consisting of two algorithms, one for analyzing worm movement and one for analysis of neural activity. Improving DIC contrast generates a dark appearance of the head, which allows head and nose tracking. Expression of GCaMP3 in only few cells, including RIS, allows automated analysis of near-continuous imaging of unrestrained worms. Together, these tools will facilitate a systematic dissection of *C. elegans* larval behavior.

RESULTS AND DISCUSSION

Automated tracking of small larvae would be desirable but has been difficult due to the weak contrast of these animals. Differential interference contrast (DIC) imaging is a classic method to image samples that have a weak contrast in bright field. The contrast is caused by changes in diffraction within the sample. DIC imaging has long been used for observing *C. elegans* and is typically employed to generate a relief-like appearance by adjusting the offset phase (Sulston and Horvitz, 1977). Our experimental strategy was to increase the contrast of our samples by optimizing DIC so that the head and the nose of the animal can be tracked automatically. For long-term imaging we cultured worms in microfluidic devices made from agarose hydrogel that were filled with bacterial food (Bringmann, 2011; Turek *et al*., 2015). We used DIC without an offset phase to generate a darkfield-like contrast. The bacteria as well as the gut of the worms have a high optical density and thus appeared bright with this contrast. The head of the worm was less optically dense and therefore appeared dark. Thus, the head was clearly visible as a dark elongated triangle over a lighter background (Fig. 1a).

As a first step to automatically tracking the behavior of the worm, we aimed to extract the head. For this, the area containing the microchamber was first cut out from the picture to mask the surrounding agar. Then, a threshold was applied and noise was reduced. Subsequently, the frame was reduced to a black background with few remaining white objects. To identify the area that corresponded to the head, the largest objects were examined for their entropy, which is lowest for the head area. Because this area defined by the threshold did not cover the entire worm head it was then treated with a closing operation that fills up small gaps in the shape and smoothens the edges. The resulting shape clearly represented the shape of the worm head (Fig. 1b).

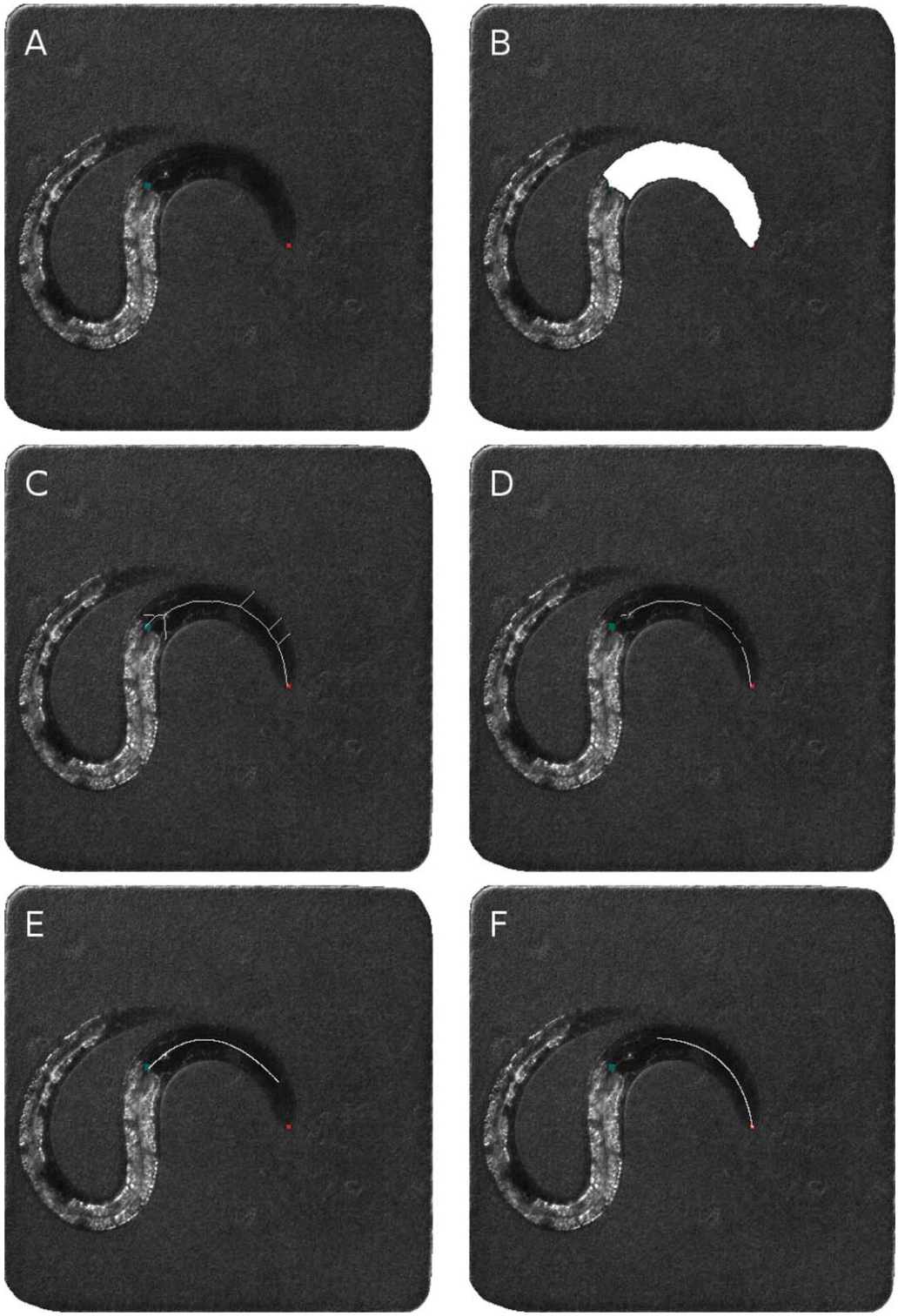

FIG. 1. An algorithm for automated tracking of larval *C. elegans* behavior using optimized DIC contrast. (**a**) DIC image before processing. The red point denotes the calculated nose position and the blue dot the back of the head. (**b**) Entropy-based identification of the head. (**c**) A skeletonization algorithm on the extracted head segment extracts the central spine of the worm head. (**d**) Removal of branching spines. (**e**, **f**) The centerline of the worm is extrapolated in both directions to find the nose tip. The previous frame determines the side on which the nose is located.

As a second step we aimed to identify the nose of the worm. To do this, we skeletonized the head shape to identify its centerline. The amount and position of branching from the resulting skeleton varied between frames. These branches needed to be reduced or removed in order to get a good approximation of the centerline of the worm head. All the different branches were disconnected from each other and were either removed or kept based on a set of filter rules. The result was a remaining skeleton that represented the centerline of the worm head (Fig. 1c). To improve the quality of the centerline, only the first half of the data points of the skeleton was kept. The other half was discarded due to the high likelihood of introducing inaccuracies from branching. With the remaining dataset a spline was calculated and a polynomial of second order was fitted onto it. The resulting function was projected onto the closed shape of the worm head and the last point of overlap between head shape and function was considered to be the best approximation to either the nose tip or back of the head. To discriminate between nose tip or back of the head we assumed that, at high frame rates (two frames per second), the new nose position is closer to the old nose position rather than the position of the back of the head. Thus, after manually assigning the nose position in few key frames, the algorithm could detect the side of the head that contained the nose accurately in subsequent frames (Fig. 1e/f).

To test the algorithm we analyzed a sample dataset with four methods: manual nose tracking, frame subtraction, automated nose tracking, head centroid tracking. We used an experiment in which sleep behavior was induced optogenetically using Channelrhodopsin activation of the RIS neuron. We used an improved version of Channelrhodopsin called ReaChR, which is activated by green to red light and which is extremely light sensitive (Lin *et al*., 2013). All analysis methods clearly detected the reduction of movement induced by RIS activation. Manual nose tracking was very precise. Automated nose tracking detected the nose in 95% of frames. It faithfully measured nose speed in the active animal and also clearly detected the reduction of nose speed after RIS activation. However, due to noise automated nose tracking was not as accurate for very low movements compared with manual tracking. Head centroid tracking correctly identified the head in 98% of frames. It systematically gave smaller movement values compared with the nose tracking because the nose is the most mobile part of the head. It appeared less noisy than automated nose tracking and clearly documented the immobilization (Fig. 2). Both nose and head centroid tracking provided an absolute quantitative readout that can be used to compare data from different settings and laboratories. Thus, we present a reliable tracking algorithm for detecting both the position of the head and nose tip, which both present reliable absolute measures for mobility. Head centroid tracking appears to be the best compromise between accuracy and analysis effort.

Understanding sleep control by RIS requires functional imaging of this neuron. Automated analysis of RIS is necessary to process the thousands of image frames that are necessary to capture its activation dynamics with high time resolution over long time periods. We used a strain that expressed the calcium sensor GCaMP3, along with the red-fluorescent protein mKate2 as an expression control, in RIS using the *aptf-1* promoter. *paptf-1::GCaMP3* expressed in RIS as well as AIB and RIB neurons. To enable automatic RIS identification, we developed an algorithm that can discriminate between RIS and other neurons. The general principle of this discrimination algorithm is that AIB and RIB are closer to the nerve ring than RIS.

First, the source image was converted into a binary image setting using a threshold. The algorithm then computed connected components. The threshold was gradually increased until the program found at least two connected components. The component with the largest area contained the nerve ring including AIB and RIB and was discarded. From the remaining components the component with the highest average brightness was chosen, which typically represents RIS.

To test the algorithm we filmed RIS activity over the sleep-wake cycle in microchambers near continuously with 0.25 frames per second and extracted RIS intensity. Because RIS activation transients typically last around 30 s, all activity transients of RIS could be captured with this protocol. In 10% of frames no RIS was detected and these frames were excluded from the analysis. Because of the high sampling rate the 90% of identified frames were sufficient to reliably track RIS activity. If needed, manual tracking of RIS would be possible for the missing frames.

Automated analysis of RIS activity showed that RIS was relatively inactive during wake behavior but acutely activated at the onset of sleep behavior. In the course of the sleep phase RIS activity decreased. Interestingly, also some activity was seen in RIS after the sleep behavior, but this RIS activity did not coincide with quiescence. Thus, a near-continuous measurement with automatic extraction of RIS activity is possible, which provides an unprecedented longitudinal view of sleep neuron activity.

Together, our methods provide a comprehensive platform for automated longitudinal analysis of single cell activity by studying RIS function in sleep control. Improved DIC contrast can be used to automatically detect head and nose movements. GCaMP-expressing neurons can be identified automatically to achieve acquisition and analysis of a near-continuous imaging of a single neuron.

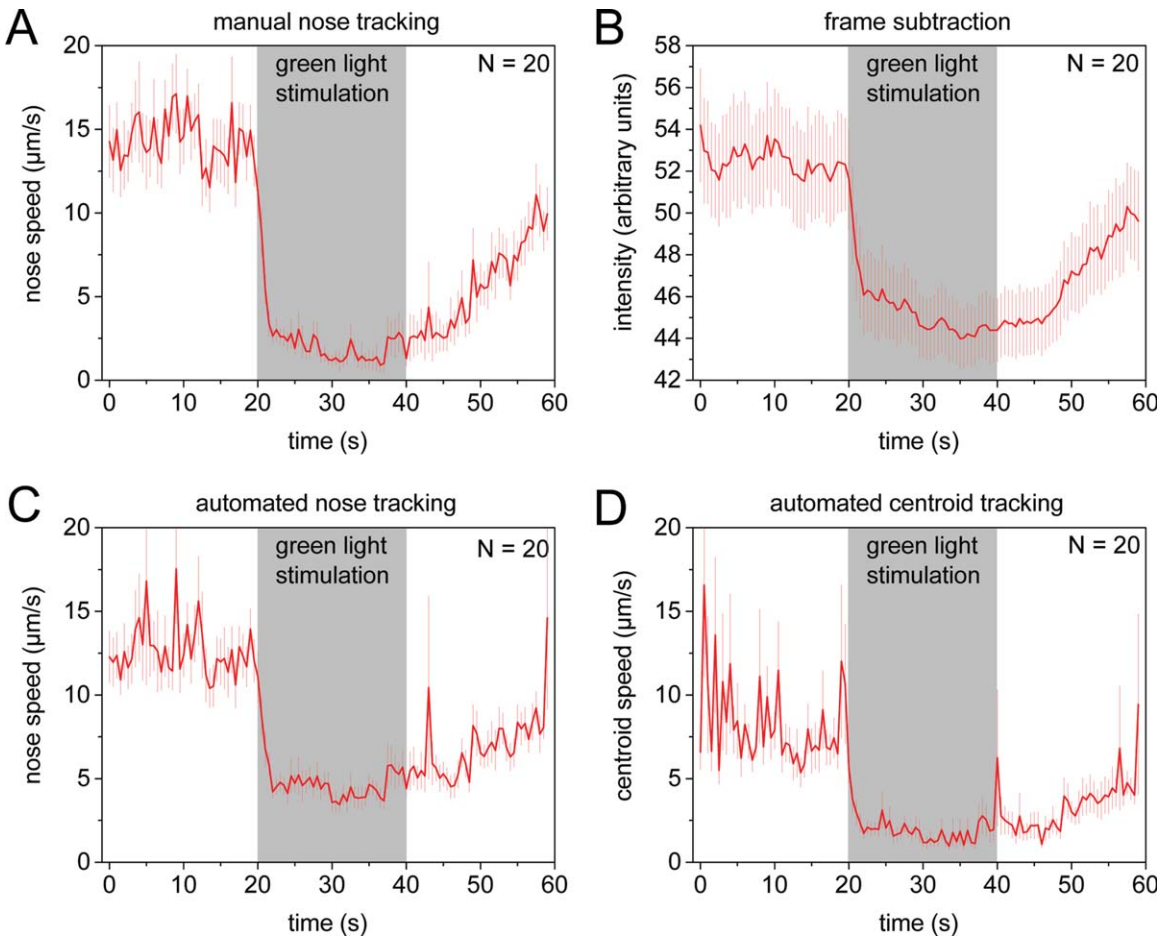

FIG. 2. Comparison of manual and automated tracking of larval *C. elegans* behavior. The effect of RIS activation was monitored in worms expressing a channelrhodopsin. RIS was activated for 20 s. Data were analyzed by (**a**) manual nose tracking, (**b**) frame subtraction, (**c**) automated nose tracking, and (**d**) automated head centroid tracking. Error bars represent SEM.

METHODS

Strains Used and *C. elegans* Maintenance

C. elegans was kept under standard conditions on NGM plates (Brenner, 1974). The ReaChR gene sequence (Lin *et al*., 2013) was optimized for expression in *C. elegans* (Redemann *et al*., 2011) and synthesized by a commercial supplier. Expression of the ReaChR transgene did not cause any detectable defect in the absence of retinal. Strains are available on request. The following strains were used:

HBR1139: *unc-119(ed3) III, goeIs261[aptf-1-5'utr::ReaChR::mKate2-aptf-1-3'utr,unc-119(+)]*.

HBR543: *unc-119(ed3) III, goeIs118[aptf-1-5'utr::SL1-GCaMP3.35-SL2::mKate2-aptf-1-3'utr,unc-119(+)]*.

HBR666: *goeIs22[pmec-4::SL1-GCaMP3.35-SL2::mKate2-unc-54-3'utr, unc-119(+)], goeIs118[aptf-1-5'utr::SL1-GCaMP3.35-SL2::mKate2-aptf-1-3'utr,unc-119(+)]*.

IMAGING

Agarose microchamber imaging was performed as described (Bringmann, 2011; Turek *et al*., 2015). Briefly, agarose chambers were cast using 3% agarose in S-basal and filled with bacteria and one pretzel-stage egg. All imaging was carried out on a Nikon TiE microscope equipped with a focus-keeping system (PFS). For DIC analysis, worms were imaged using a 40× oil objective and a Neo sCMOS camera (Andor). Adult hermaphrodites were grown on NGM plates supplemented with 0.2 mM all trans retinal (Sigma). Eggs from these mothers were placed into microchambers for analysis. Stimulation of Channelrhodopsin was done using an LED of 585 nm with 10^{-4} mW/mm^2.

For fluorescence analysis, worms were filmed with a 20× objective and an EMCCD camera (Andor). For fluorescence, LED light was TTL-triggered to match the exposure of the camera. Stimulation of GCaMP was

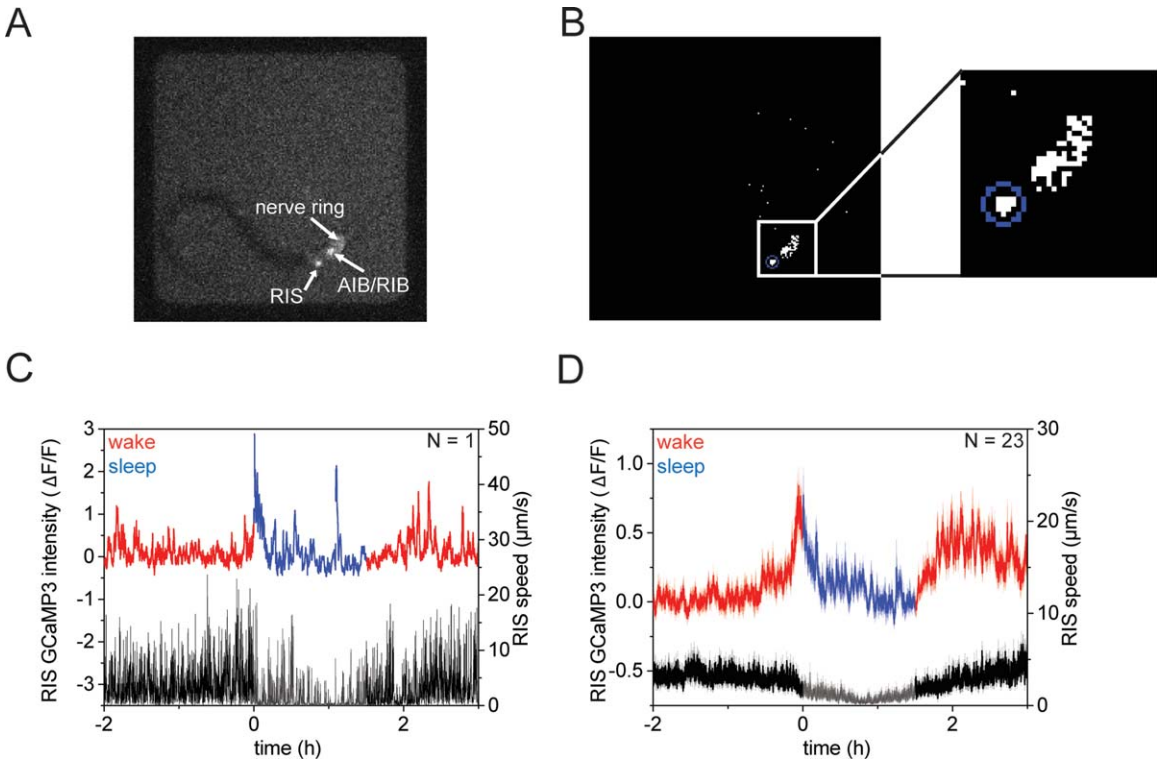

FIG. 3. Automated analysis of sleep neuron activity with near-continuous imaging over long time scales. RIS activity was measured over the sleep–wake cycle in worms expressing GCaMP3. (**a**) GCaMP signals were obtained for AIB, RIB, and RIS. (**b**) Automatic identification of RIS. (**c**) RIS activity for an individual animal. (**d**) Averaged RIS activity for several animals. Red shows RIS activity in wake and blue during sleep. As a measure of mobility, the movement data of the RIS neuron was plotted for wake (black) and for sleep (gray). For this, the center position of the RIS neuron, as determined by automated RIS tracking, was used to calculate movement speed. Error bars represent SEM.

done using an LED of 490 nm with 2.8 mW/mm^2. A frame was taken every 4 s for 12 h.

ANALYSIS OF DIC IMAGES

For automated tracking a program was written in python (Python Software Foundation. Python Language Reference, version 3.4.3. Available at http://www.python.org). Important modules used for the algorithm that were not part of the Python standard library were: *scikit-image* for image processing (van der Walt *et al.*, 2014), *matplotlib* for creating graphs (Hunter, 2007), *numpy* to handle arrays (van der Walt *et al.*, 2011), and *scipy* for image handling and extrapolation (Jones et al. SciPy: Open Source Scientific Tools for Python, 2001, http://www.scipy.org/[Online; accessed 2015-11-17]).

Because the corners of the chamber were slightly rounded, these round edges were removed using edge detection with the *scikit-image* module. Gauss filtering was done using the *scipy* module. Optimal threshold settings depended on the brightness of the image and thus were variable. A Monte Carlo-based algorithm was used to quickly approximate the optimal threshold for the empirically defined head size for each frame (Metropolis and Ulam, 1949). Entropy determination, skeletonization operation, and the medial axis transform algorithm were done with the *scikit-image* module. The second order polynomial was fitted with the *scipy* module. The analysis package is available online at http://pubman.mpdl.mpg.de/pubman/faces/viewItemFullPage.jsp?itemId = escidoc:2230994:2 (http://hdl.handle.net/11858/00-001M-0000-0029-1E24-9 direct link).

ANALYSIS OF RIS ACTIVITY

We wrote a Matlab script for automatically tracking the RIS using standard Matlab functions. The script is executed using a user set initial threshold. The threshold should be set low but significantly higher than zero. Setting everything above the threshold to 1 creates a binary representation of the image. From the binary image the connected components are extracted and the area and average intensity are determined. If at least two components are found and the sum of the areas occupied by the components is sufficiently big the function uses the found components as possible candidates for RIS. If the requirements are not met, the threshold is gradually increased and the process is repeated until the requirements are met or the process is repeated for a maximum of nine times. In case the

script is not able to find the RIS in the current picture the procedure is terminated. If possible candidates exist, the component occupying the largest area represents the nerve ring including the other neurons and is discarded. From the remaining components the area with the highest intensity is chosen. This area is discarded if it is located closely to the edge of the image. This selection criterion is necessary due to possible unexpected behavior of the function for candidates close to the image edge. If the area is not close to the edge it is assumed to be RIS. The algorithms also detected RIS when additional neurons were present (*mec-4*-expressing neurons, HBR666, used for Fig. 3c/d). The matlab script is available on request.

ACKNOWLEDGMENTS

We thank Andre Brown for the idea of using entropy to identify the head, Boris Busche for advice on DIC image processing, and Edmund Henniges for help with Matlab.

REFERENCES

Bringmann H. 2011. Agarose hydrogel microcompartments for imaging sleep- and wake-like behavior and nervous system development in *Caenorhabditis elegans* larvae. J Neurosci Methods 201:78–88.

Campbell SS, Tobler I. 1984. Animal sleep: A review of sleep duration across phylogeny. Neurosci Biobehav Rev 8:269–300.

Cassada RC, Russell RL. 1975. The dauerlarva, a post-embryonic developmental variant of the nematode *Caenorhabditis elegans*. Dev Biol 46:326–342.

Cho JY, Sternberg PW. 2014. Multilevel modulation of a sensory motor circuit during *C. elegans* sleep and arousal. Cell 156:249–260.

Cirelli C, Tononi G. 2008. Is sleep essential? PLoS Biol 6: e216.

Hill AJ, Mansfield R, Lopez JM, Raizen DM, Van Buskirk C. 2014. Cellular stress induces a protective sleep-like state in *C. elegans*. Curr Biol 24:2399–2405.

Hunter JD. 2007. Matplotlib: A 2D graphics environment. Comput Sci Eng 9:90–95.

Iwanir S, Tramm N, Nagy S, Wright C, Ish D, Biron D. 2013. The microarchitecture of *C. elegans* behavior during lethargus: Homeostatic bout dynamics, a typical body posture, and regulation by a central neuron. Sleep 36:385–395.

Jeon M, Gardner HF, Miller EA, Deshler J, Rougvie AE. 1999. Similarity of the *C. elegans* developmental timing protein LIN-42 to circadian rhythm proteins. Science 286:1141–1146.

Kerr R, Lev-Ram V, Baird G, Vincent P, Tsien RY, Schafer WR. 2000. Optical imaging of calcium transients in neurons and pharyngeal muscle of *C. elegans*. Neuron 26:583–594.

Kerr RA. 2006. Imaging the activity of neurons and muscles. WormBook 1–13.

Lin JY, Knutsen PM, Muller A, Kleinfeld D, Tsien RY. 2013. ReaChR: A red-shifted variant of channelrhodopsin enables deep transcranial optogenetic excitation. Nat Neurosci 16:1499–1508.

Metropolis N, Ulam S. 1949. The Monte Carlo method. J Am Stat Assoc 44:335–341.

Nagy S, Raizen DM, Biron D. 2014. Measurements of behavioral quiescence in *Caenorhabditis elegans*. Methods 68:500–507.

Raizen DM, Zimmerman JE, Maycock MH, Ta UD, You YJ, Sundaram MV, Pack AI. 2008. Lethargus is a *Caenorhabditis elegans* sleep-like state. Nature 451: 569–572.

Redemann S, Schloissnig S, Ernst S, Pozniakowsky A, Ayloo S, Hyman AA, Bringmann H. 2011. Codon adaptation-based control of protein expression in *C. elegans*. Nat Methods 8:250–252.

Roffwarg HP, Muzio JN, Dement WC. 1966. Ontogenetic development of the human sleep-dream cycle. Science 152:604–619.

Saper CB, Scammell TE, Lu J. 2005. Hypothalamic regulation of sleep and circadian rhythms. Nature 437: 1257–1263.

Schwarz J, Bringmann H. 2013. Reduced sleep-like quiescence in both hyperactive and hypoactive mutants of the Galphaq Gene egl-30 during lethargus in *Caenorhabditis elegans*. PLoS One 8: e75853.

Schwarz J, Lewandrowski I, Bringmann H. 2011. Reduced activity of a sensory neuron during a sleep-like state in *Caenorhabditis elegans*. Curr Biol 21: R983–R984.

Schwarz J, Spies JP, Bringmann H. 2012. Reduced muscle contraction and a relaxed posture during sleep-like lethargus. Worm 1:12–14.

Singh K, Ju JY, Walsh MB, DiIorio MA, Hart AC. 2014. Deep conservation of genes required for both *Drosophila melanogaster* and *Caenorhabditis elegans* sleep includes a role for dopaminergic signaling. Sleep 37:1439–1451.

Sulston JE, Horvitz HR. 1977. Post-embryonic cell lineages of the nematode, Caenorhabditis elegans. Dev Biol 56:110–156.

Turek M, Besseling J, Bringmann H. 2015. Agarose microchambers for long-term calcium imaging of *Caenorhabditis elegans*. J Vis Exp e52742.

Turek M, Lewandrowski I, Bringmann H. 2013. An AP2 transcription factor is required for a sleep-active neuron to induce sleep-like quiescence in *C. elegans*. Curr Biol 23:2215–2223.

Van Buskirk C, Sternberg PW. 2007. Epidermal growth factor signaling induces behavioral quiescence in *Caenorhabditis elegans*. Nat Neurosci 10:1300–1307.

van der Walt S, Colbert SC, Varoquaux G. 2011. The NumPy array: A structure for efficient numerical computation. Comput Sci Eng 13.

van der Walt S, Schonberger JL, Nunez-Iglesias J, Boulogne F, Warner JD, Yager N, Gouillart E, Yu T. 2014. scikit-image: Image processing in Python. Peer J 2:e453.

Yemini E, Jucikas T, Grundy LJ, Brown AE, Schafer WR. 2013. A database of *Caenorhabditis elegans* behavioral phenotypes. Nat Methods 10:877–879.

You YJ, Kim J, Raizen DM, Avery L. 2008. Insulin, cGMP, and TGF-beta signals regulate food intake and quiescence in *C. elegans*: A model for satiety. Cell Metab 7:249–257.